

Electrooxidation of glucose by binder-free bimetallic Pd₁Pt_x/graphene aerogel/nickel foam composite electrodes with low metal loading in basic medium

Chi-Him A. Tsang^a, K.N. Hui^{b*}, K.S. Hui^{c*}

^a Department of System Engineering and Engineering Management, City University of Hong Kong, Hong Kong

^b Institute of Applied Physics and Materials Engineering, University of Macau, Avenida da Universidade, Macau

^c School of Mathematics, University of East Anglia, Norwich, NR4 7TJ, United Kingdom

*Corresponding author

E-mail address: bizhui@umac.mo (K.N. Hui)

E-mail address: k.hui@uea.ac.uk (K.S. Hui)

Abstract

Many 2D graphene-based catalysts for electrooxidation of glucose involved the use of binders and toxic reducing agents in the preparation of the electrodes, which potentially causes the masking of original activity of the electrocatalysts. In this study, a green method was developed to prepare binder-free 3D graphene aerogel/nickel foam electrodes in which bimetallic Pd-Pt NP alloy with different at% ratios were loaded on 3D graphene aerogel. The influence of Pd/Pt ratio (at%: 1:2.9, 1:1.31, 1:1.03), glucose concentration (30 mM, 75 mM, 300 mM, 500 mM) and NaOH concentration (0.1 M, 1 M) on electrooxidation of glucose were investigated. The catalytic activity of the electrodes was enhanced with increasing the Pd/Pt ratio from 1:2.9 to 1:1.03, and changing the NaOH/glucose concentration from 75 mM glucose/0.1 M NaOH to 300 mM glucose/1 M NaOH. The Pd₁Pt_{1.03}/GA/NF electrode achieved a high current density of 388.59 A g⁻¹ under the 300 mM glucose/1 M NaOH condition. The stability of the electrodes was also evaluated over 1000 cycles. This study demonstrated that the Pd₁Pt_{1.03}/GA/NF electrode could be used as an anodic electrode in glucose-based fuel cells.

Keyword: Palladium, platinum, graphene aerogel, glucose cell

1. Introduction

The direct oxidation of glucose for electrical energy generation in fuel cell has been widely investigated in previous decades due to its abundance, high energy density, non-toxic, cheap, easy handling, and renewability.[1-5] More importantly, glucose can be extracted from either biomass waste in agricultural activity or dedicated energy crops, which made it an attractive fuel in fuel cell applications.[3, 6]

Development on the metallic catalysts for glucose electro-oxidation has been extensively studied in the past few decades in order to obtain a good combination of metal catalysts with the glucose and the electrolyte concentrations.[1-5] Among them, Pt and Pd based catalyst were the most commonly investigated candidates due to their strong electrocatalytic activity in alcohol and glucose oxidation.[7-13] Polymetallic materials, such as bimetallic alloy, are the most popular catalytic materials for electrooxidation of glucose in past decades because they show enhanced catalytic ability than the monometallic one.[10, 13] Among them, bimetallic Pd based alloys were the most commonly used catalyst for glucose fuel cells. Pd/Rh, Pd/Ni, Pd/Au, and Pd/Pt, were loaded on different substrates like Ppy,[14] carbon,[2, 6, 15, 16] and 2D graphene,[17] which showed high catalytic activity in glucose electrooxidation.

Recently, 2D graphene nanosheets (GNS) based materials have been evaluated for different applications in energy,[18, 19] chemical sensing,[17, 20, 21] photoconductive switch,[22] catalysts of chemical reaction,[23, 24] and biomedical imaging and biosensing [25, 26] due to the large surface area provided by 2D GNS for stabilizing metal nanoparticles.[7, 23, 27-29] Different methods were developed for the preparation of binder-free 2D GNS based fuel cell electrodes.[12, 30] Recently, 3D structured graphene aerogel (GA) has attracted a new focus due to the presence of 3D cross-linked network of GNS. Monometallic Pd loaded GA/NF (Pd/GA/NF)

electrode was developed through a green and one-step preparation, which showed a high electrocatalytic activity and stability in alcohol oxidation.[31]

Many works have been conducted to enhance the overall activity of bimetallic catalysts on different substrates in glucose electrooxidation under a Pd:M (M: Pt, Ph) ratio of 1:1 (at%) [2, 14, 17] at fixed glucose solution concentration (5 mM, 20 mM, 500 mM, or 0.1 M).[2, 14, 17] In addition, other works showed that a good performance in glucose oxidation was obtained at different ratios of 2 metals not equal to 1:1 (Pd₁Pt_{0.37}, Pd₃₀Au₇₀, and Au₉₅Ru₅).[13, 15, 32] In case of the metal-loaded graphene catalyzed glucose electrooxidation research, most of the study was related to the glucose sensing,[17, 33, 34] the study focused on their electrocatalytic activity in the glucose electrooxidation was relatively few in number.[35, 36] Moreover, most of the activity study was focused on the single cycle activity only, [2, 13-15, 17, 35] the systematic study in influence of glucose and hydroxide (OH⁻) concentrations on the glucose electrooxidation of the metal-loaded catalytic electrodes was relatively few in number,[2, 6] graphene based one with long term stability together was even rare.[36] It is expected that highly stable bimetallic catalysts are important for prolong glucose electrooxidation.

Herein, we investigated the catalytic performance of binder-free bimetallic Pd-Pt alloy loaded GA/NF electrodes with different Pd/Pt ratios (at%: 1:2.9, 1:1.31, and 1:1.03) in glucose electrooxidation under different concentrations of NaOH (0.1 M and 1 M) and glucose (30 mM to 500 mM) at room temperature. The long term stability of the Pd-Pt/GA/NF electrodes was also investigated.

2. Experimental

2.1. Materials

The macroporous Ni foam (NF; 110 pore per inch; mass density of 320 g m⁻², Artenano Company Limited, Hong Kong), potassium hexachloropalladate (IV) (K₂PtCl₆, 99.9999%, Sigma-Aldrich), potassium hexachloroplatinate (IV) (K₂PtCl₆, 99.9999%, Sigma-Aldrich), Vitamin C (VC, Hwa Da Chemical), glucose (99.9%, Sigma-Aldrich), and sodium hydroxide (NaOH, 99.9%, Sigma-Aldrich) was used directly as received. All aqueous solutions were prepared with Milli-Q water.

2.2. Pd-Pt/GA/NF preparation

The GO was prepared through modified Hummer's method according to the previous literature.[37] The bimetallic alloy loaded GA was prepared through a modified chemical reduction method.[18, 31] Briefly, 180 mg of freeze dried GO was dispersed in 30 ml DI water for few minutes in order to produce 6 mg ml⁻¹ GO dispersion. Fixed amount (120 mg) of K₂PdCl₆ and various amounts (145.8 mg, 72.9 mg or 48.6 mg) of K₂PtCl₆ (molar ratio of Pd:Pt=1:1, 2:1 or 3:1) was added to 6 mg ml⁻¹ GO dispersion and stirred for at least 30 min under room temperature in order to ensure well mixing between Pd, Pt, and GO for the formation of 10 mM:10 mM (1:1), 10 mM:5 mM (2:1) or 10 mM:3.33 mM (3:1) Pd-Pt/GO mixture. The cleaned porous NF strip (10 cm×0.5 cm×0.2 cm) was immersed into the well mixed Pd-Pt/GO dispersion with ultrasonic treatment for 20 min, followed by aging at room temperature for 2 h. The Pd-Pt/GO soaked NF was then transferred to a bottle containing 0.5 g VC (143 mM, 20 cm³) solution and then kept at 60 °C at 48 h without stirring to facilitate the formation of bimetallic Pd-Pt/graphene hydrogel (GH) on NF. The as-prepared Pd-Pt/GH/NF was cleaned by soaking the whole strip in DI water for 3 days in order to remove the residue VC, PdCl₆²⁻ and PtCl₆²⁻. The cleaned Pd-Pt/GA/NF was obtained by freeze-drying the Pd-Pt/GH/NF strip at 48 h under vacuum. Based on the XRF analysis (Table S1), Pd₁Pt_{2.9}/GA/NF (at% based) was

produced from 1:1 PdCl₆²⁻/PtCl₆²⁻ mixture in the process. Similarly, Pd₁Pt_{1.31}/GA/NF, and Pd₁Pt_{1.03}/GA/NF were prepared with 2:1 PdCl₆²⁻/PtCl₆²⁻ mixture, and 3:1 PdCl₆²⁻/PtCl₆²⁻ mixture in the synthesis, respectively.

2.3. Characterization

The optical image of the electrode was obtained from using a stereo microscope (Olympus SZX12). The SEM/EDX analysis of the electrodes was performed through the SEM system (JEOL-JSM5600). The TEM analysis of the samples scratched from electrodes was performed through the TEM system (Philips FEI Tecnai G2 20 S-Twin Scanning TEM). The X-Ray diffraction (XRD) was obtained with aqueous dispersion of sample powder on X-Ray diffractometer (Philips Xperts') using Cu K α radiation ($\lambda=0.154$ nm). XRD pattern was recorded from 5° to 95° with scanning rate of 0.01°s⁻¹. The surface elemental information of electrodes was determined by X-Ray Photoelectron Spectroscopy system (XPS, Physical Electronics PHI Model 5802) at room temperature. The bulk elemental composition of electrodes was determined an X-Ray Fluorescence spectrometer (Eagle III-EDAX).

2.4. Electrochemical characterization of the Pd-Pt/GA/NF electrode

The electrochemical characterization was performed by CHI660D electrochemical workstation through cyclic voltammetry (CV) with 3-electrode system.[10, 38, 39] Freeze-dried Pd-Pt/GA/NF electrodes with different Pd/Pt ratios were used as the working electrode directly without further treatment. Standard calomel electrode (SCE: Hg/HgCl₂) and a Pt wire were used as the reference electrode, and the counter electrode, respectively. The catalytic performance of the electrodes were evaluated in 30 mM, and 75 mM glucose in 0.1 M NaOH, and 75 mM, 300 mM, and 500 mM glucose in 1 M NaOH with scanning rate of 0.05 V s⁻¹ and scanning

range of -1.145 to +0.955 V against SCE, which are the common conditions used in direct glucose fuel cells.[2, 6, 13, 14, 40-42] The mean values along with standard deviations (within $\pm 5\%$) of 3 sets of independent experiments are reported.

3. Results and discussions

3.1. Characterization of Pd-Pt/GA/NF electrodes

After the freeze-dry treatment, a black electrode was obtained (Figs. S1a and S1b, supplementary information). Fig. 1 shows the SEM and EDX results of the Pd₁Pt_{2.9}/GA/NF electrode (based on XRF analysis, Table S1). Fig. 1a showed that the NF was composed of 3D macroporous Ni network. In Figs. 1b-d, the Pd-Pt/GA was covered and filled into the pores of the NF skeleton, which indicated that the Pd-Pt/GO dispersion was filled into the pores of the NF in the aging stage. The Pd-Pt NPs loaded on the GA reflected that the reduction of PdCl₆²⁻, PtCl₆²⁻, and GO by VC solution was achieved. The presence of the Pd-Pt NPs was confirmed from the strong Pt and weak Pd signals in the EDX spectrum (Fig. 1e). Further analysis of EDX elemental mapping of the Pd-Pt/GA/NF electrodes was also performed (Fig. S2). The results showed that similar homogenous Pd L α -1 and Pt M α -1 patterns were observed and matched to the particle pattern in the corresponding SEM images, which indicated the formation of Pd/Pt alloy particles on the GA.[43, 44] In addition, the C K α -1 pattern was similar to the corresponding SEM images, which reflected the presence of graphene in the GA. Further characterization through TEM (Fig 2a-b) showed that the bimetallic Pd-Pt NPs was deposited on the graphene nanosheets surface with spherical and square shapes. The SAED (Fig 2c) results showed that the Pd-Pt NPs have hexagonal SAED pattern, the information from Table S2 showed that the d-spacing of 3 spots in Fig 2c were 2.274 Å, 2.251 Å, and 1.97 Å respectively, which were corresponding to (111), (111), and (200) faces respectively. Base on the reference

data of monometallic Pd (JPCDS card No. 46-1043) and Pt (JPCDS card No. 04-0802), it primarily showed that bimetallic Pd-Pt NPs in Pd₁Pt_{2.9}/GA/NF composite have f-c-c crystal structure with high crystallinity.

XRD is one of the powerful characterization techniques for the presence of Pd-Pt alloy materials on the Pd-Pt/GA/NF electrodes. From the XRD spectra obtained in Fig S3, the presence of Pd signal pattern was the evidence of successful loading of Pd onto the GA. The position of Pd 2 θ peaks at 40°, 47°, 68°, 82° were assigned to the Pd (111), Pd (200), Pd (220), and Pd (311) respectively, while those of Pt 2 θ peaks (39.95°, 16.7°, 68.2°, and 81.6°) were assigned as Pt (111), Pt (200), Pt (220), and Pt (311). The result showed that monometallic Pd NPs and Pt NPs have f-c-c structure (JPCDS card No. 46-1043 and 04-0802) with high crystallinity.[10] From the magnified view of M (111) of the Pd-Pt/GA samples (Fig. S3b), it showed that the peak position was lied between that of monometallic Pd and Pt respectively. Based on the reported literatures[10] and the SAED results from Fig 2c and Table S2, the crystal face reflected from the d-spacing was highly matched with the XRD metal peak pattern ($2\theta=39-90^\circ$). This proved that the NPs were Pd-Pt alloy particle in nature with f-c-c crystal structure. Meanwhile, the diffraction peaks were 10° in the GO (Fig. S3a), and 11.85-13° in Pd/GA, corresponding to the interlayer distance of 8.84 Å and 7.46 Å, respectively. The reduction on the interlayer distance in GA relative to the GO revealed that the reduction of oxide functional groups by VC was taken place.[45]

We further analyzed the Pd-Pt/GA samples through XPS. From the XPS spectra obtained in Figs. 3 and S4, the presence of twin Pd and Pt signal peaks in Pd3d and Pt4f spectra was the evidence of bimetallic Pd-Pt loaded onto the GA. In the Ni2p spectrum (Fig. 3a), major Ni peak (856.03 eV) and its satellite peak (861.4 eV) were observed. In the Pt4f spectrum (Fig. 3b), the strong signals at 71.03 eV and 74.32 eV were corresponded to Pt⁰, and the weak signals at 71.60 eV and 74.80 eV, and 75.60

eV and 77.70 eV (shoulder peaks) were assigned to Pt^{2+} and Pt^{4+} , respectively. The strong signals at 335.2 and 340.4 eV and weak signals at 337.3 and 342.6 eV (shoulder peaks) were obvious observed in Pd3d spectrum (Fig. 3c). By comparing with the reference spectra of Pd-Pt loaded graphene nanosheets,[10, 43, 44] the signal positions in the current samples were very close to the reference data, which showed that the 2 twin signals were corresponding to Pd^0 and Pd^{2+} respectively. The shape of Pd, Pt signals was also independent to the Pd/Pt ratios (Figs. 3 and S4), which are similar to the study.[46] In addition, in the C1s spectra (Fig. 3d), signals at 284.3, 286.1 (shoulder peak), 288.3 and 288.8 (shoulder peak) eV were observed, which reflected that those peaks were C-C, -C-OH, -O-C-O-, and O=C-OH groups respectively.[7] GO (Fig. 3e) was reduced into graphene due to reduction in the oxidized carbon group's peak intensity.[7] By comparing the C1s spectrum of the reported Ni loaded carbon species with our samples (Fig 3d, S4g, S4h), the Ni-C signal peak at 281-282 eV was not observed,[47] which showed that no Ni-C bond was formed during the mild conditioned reduction. Such finding suggests that NF was acted as a substrate only in the simultaneous reduction of Pd/Pt and GO during the $\text{Pd}_1\text{Pt}_x/\text{GH}$ formation on the NF surface without direct chemical reaction between GO and NF.

3.2. Electrochemical characterization

3.2.1. Electro-oxidation activity of Pd-Pt/GA/NF electrodes in alkaline glucose solution

The electrocatalytic activity of the electrodes in 30 mM glucose/0.1 M NaOH solution was investigated. The effective mass of Pt/Pd alloy NPs on the electrodes was 2.8 mg ($\text{Pd}_1\text{Pt}_{2.9}$), 1.8 mg ($\text{Pd}_1\text{Pt}_{1.31}$), and 0.2 mg ($\text{Pd}_1\text{Pt}_{1.03}$), respectively. In Fig. 4, three peaks were observed in the CV at the 25th cycle. The 25th cycle was chosen as

the shape of CV curve at that cycle had no significant difference within 50-100 cycles. The peak at -0.476 to -0.396 V in forward scan (a1) was due to oxidation of glucose by the Pd-Pt/GA/NF electrodes, another peak at +0.244 to +0.284 V (a2) was due to oxidation of glucose acid or gluconolactone produced from the glucose oxidation at a1 peak (-0.4 to -0.48 V), while the peak at -0.414 V in reverse scan was due to oxidation of CO on the surfaces of bimetallic catalyst.[36] The shape of CV curves were similar to the reported studies.[13, 48]

For the Pd₁Pt_{2.9}/GA/NF electrode, the peak current density (J_f : A g⁻¹) was 6.24 A g⁻¹ (a1) and 10.26 A g⁻¹ (a2) in forward scan, while that in the reverse scan (J_b) was -0.979 A g⁻¹. When the Pd/Pt ratio increased to 1:1.31, J_f and J_b were slightly increased to 15.74 A g⁻¹ (a1) and 26.06 A g⁻¹ (a2) and -0.798 A g⁻¹, respectively. The value of J_f and J_b was sharply increased to 82.02 A g⁻¹ (a1), 116.4 A g⁻¹ (a2) and -0.251 A g⁻¹ when Pd/Pt ratio further increased to 1:1.03. The results indicated that the electrochemical activity of the electrodes in glucose oxidation was increased when Pd/Pt ratio increased from 1:2.9 to 1:1.03, which was in agreement with a study of using Pd/Pt catalysts in glucose sensing.[17] By comparison to the values of J_f recorded from the monometallic Pd/GA electrode (a1: 5.08 A g⁻¹, a2: 8.63 A g⁻¹) and the Pt/GA electrode (a1: 2.89 A g⁻¹, a2: 4.29 A g⁻¹), the J_f recorded were increased due to the synergistic effect of Pd and Pt (particularly in Pd/Pt ratio near 1:1) in glucose oxidation in which Pd improved the electronic structure of Pt,[13, 36] which reflected on the shifting of the M(111) peak position in the XRD spectrum of the bimetallic Pd₁Pt_x/GA against monometallic Pd/GA and Pt/GA (Fig S3b) in certain extent. This phenomenon was more obvious when the Pd/Pt at% ratio approaching to 1:1,[13] which was similar to our case based on the CV results of the glucose electrooxidation mentioned in Table 1 and the XRF results on the sample composition described in Table S1.

3.2.2. Effect of NaOH concentration

Based on the proposed mechanism of glucose electrooxidation [13, 42], Pd was the main reaction site:[13]

Step 1 Pd+Glucose→Pd-H+Intermediates

Step 2 Pd+xOH⁻→Pd(OH)_x+xe⁻

Step 3 Pd(OH)_x+Intermediates→Pd+Glucolactone/Gluconic acid

Step 4 Pd(OH)_x+Glucose→Pd+Glucolactone/Gluconic acid

Glucose and OH⁻ played an important role in glucose electrooxidation process. As the result, the influence of NaOH concentration on electrocatalytic activity of the electrodes was firstly investigated at glucose concentration of 75 mM (Table 1). The activity of electrodes at 75 mM glucose/0.1 M NaOH was presented in Fig. S5a and Table 1, with the peak current density values of 2.84 A g⁻¹ (Pd₁Pt_{2.9}), 4.86 A g⁻¹ (Pd₁Pt_{1.31}), 13.33 A g⁻¹ (Pd₁Pt_{1.03}) for a1 peak; and 6.20 A g⁻¹ (Pd₁Pt_{2.9}), 10.46 A g⁻¹ (Pd₁Pt_{1.31}), 28.1 A g⁻¹ (Pd₁Pt_{1.03}) for a2 peak, respectively. When the concentration of NaOH increased to 1 M (Fig. S5b and Table 1), the sharpness of peaks was increased. When the Pd/Pt ratio was 1:2.9, the J_f of 2 redox peaks was 15.83 A g⁻¹ (-0.696 V, a1) and 26.76 A g⁻¹ (-0.156 V, a2), and the J_b of reverse scan was 5.51 A g⁻¹. When the Pd/Pt ratio increased to 1:1.31, the value of J_f (2 peaks) and J_b was slightly increased to 19.9 A g⁻¹ (-0.776 V, a1), 29.3 A g⁻¹ (-0.016 V, a2), and 8.81 A g⁻¹, respectively. The value of J_f and J_b was further increased sharply to 71.33 A g⁻¹ (-0.776 V, a1), 94.78 A g⁻¹ (-0.076 V, a2), and 49.65 A g⁻¹ (-0.334 V), respectively when the Pt/Pt ratio further increased to 1:1.03. The redox peaks were clearly shown than that in 0.1 M NaOH solution. Generalized results above mentioned shows that the higher the NaOH concentration, the more obvious the redox peaks intensity in the forwards scan of glucose oxidation when the NaOH concentration increases from 0.1 M to 1 M.

In general case, the increase in the OH^- concentration beyond the optimum concentration enhances the electrocatalytic activity of the electrodes due to the enhancement in catalytic kinetics in glucose electrooxidation under constant glucose concentration. Such observation was probably resulted from the increased amount of highly mobile OH^- which enhanced the interaction with the adsorbed glucose molecules in the solution, leading to the increase in the electrochemical kinetics.[2, 6, 36] The results above mentioned indicated that glucose oxidation can be accelerated by the presence of OH^- anions, leading to an increase in the anodic peak.[2, 6, 36]

3.2.3. Effect of glucose concentration

The electrocatalytic activity of the electrodes in different glucose concentrations at 1 M NaOH concentration was then investigated (Figs. 6 and S6, and Table 1). In Figs. 6a and S6a, for the $\text{Pd}_1\text{Pt}_{2.9}/\text{GA}/\text{NF}$ electrode, increasing glucose concentration from 75 mM to 300, two sharp peaks in forward scans (J_f values of 19.40 A g^{-1} (a1), 43.92 A g^{-1} (a2)) and one peak (J_b value of 20.34 A g^{-1}) in reverse scan were obtained. However, the peak intensities were reduced when the glucose concentration was further increased to 500 mM. When the Pd/Pt ratio of the Pd-Pt/GA/NF electrodes increased to 1:1.31 and 1:1.03, similar observations were obtained as in the $\text{Pd}_1\text{Pt}_{2.9}/\text{GA}/\text{NF}$ electrode (Figs. 6b-6c, S6b). However, the peak positions in both forward and reverse scan were shifted towards positive potential when NaOH concentration was fixed at 0.1 M, as shown in Fig. 7. In addition, the peak intensity was reduced upon the increase in glucose concentration. The J_f values were reduced from 6.24 A g^{-1} ($\text{Pd}_1\text{Pt}_{2.9}$), 15.74 A g^{-1} ($\text{Pd}_1\text{Pt}_{1.31}$), 82.02 A g^{-1} ($\text{Pd}_1\text{Pt}_{1.03}$) for a1 peak; and 10.26 A g^{-1} ($\text{Pd}_1\text{Pt}_{2.9}$), 26.06 A g^{-1} ($\text{Pd}_1\text{Pt}_{1.31}$), 116.4 A g^{-1} ($\text{Pd}_1\text{Pt}_{1.03}$) for a2 peak in 30 mM glucose/0.1 M NaOH, to 2.84 A g^{-1} ($\text{Pd}_1\text{Pt}_{2.9}$), 4.86 A g^{-1} ($\text{Pd}_1\text{Pt}_{1.31}$), 13.33 A g^{-1} ($\text{Pd}_1\text{Pt}_{1.03}$) for a1 peak; and 6.20 A g^{-1} ($\text{Pd}_1\text{Pt}_{2.9}$), 10.46 A g^{-1} ($\text{Pd}_1\text{Pt}_{1.31}$), 28.1 A g^{-1} ($\text{Pd}_1\text{Pt}_{1.03}$) for a2 peak.

g^{-1} ($\text{Pd}_1\text{Pt}_{1.03}$) for a2 peak in 75 mM glucose/0.1 M NaOH, which were similar to the results in Fig. 6. It is expected that the catalytic performance of the electrodes could be enhanced under higher glucose concentration under constant NaOH concentration (with improved kinetics of electrooxidation of glucose) before reaching the optimum glucose concentration.[2, 6, 36] However, further increase in the glucose concentration may leads to a difficulty in adsorption of OH^- on the active sites. As a result, the overall electrochemical kinetics was lowered, which is in agreement with the literature.[2, 6, 36] Based on the results, the Pd-Pt/GA/NF electrodes showed the best performance at the 300mM glucose/1M NaOH condition.

3.2.4. Stability study

The stability of the Pd-Pt/GA/NF electrodes was then evaluated in 300mM glucose/1 M NaOH solution through CV with 1248 cycles. CV spectra of Pd-Pt/GA/NF electrodes, the variation of J_f and onset potential of the electrodes were summarized in Fig. 8 and Tables S3-S5, respectively. The variation of J_f (from a2 peak) was more obvious than that of a1 peak (Tables S3-S5), which was due to the electrodes exhibited higher sensitivity in oxidation of intermediate species which were generated from glucose oxidation.[48] Thus, variation of a2 peak was used in this study. In the $\text{Pd}_1\text{Pt}_{2.9}$ /GA/NF electrode (Fig 8a), the maximum $J_f(\text{a2})$ value of 43.9 A g^{-1} was recorded at 25th cycle. The $J_f(\text{a2})$ decreases with increasing number of cycles. The $J_f(\text{a2})$ value was reduced to 13.34 A g^{-1} at 1248th cycle, resulted in 69.6% loss of activity (Table S2). When the Pd/Pt ratio increased to 1:1.31 (Fig 8b), the maximum $J_f(\text{a2})$ of 80.3 A g^{-1} was recorded at 100th cycles. The $J_f(\text{a2})$ was reduced to 14.03 A g^{-1} at 1248th cycle, resulted in 82.5% loss of activity (Table S4). When the Pd/Pt ratio further increased to 1:1.03 (Fig 8c), the maximum $J_f(\text{a2})$ of 388.59 A g^{-1} was recorded at 50th cycle. The $J_f(\text{a2})$ was reduced to 80.42 A g^{-1} at 1248th cycle, resulted in 79.3%

loss of activity (Table S5). The reason is that the products of glucose oxidation were adsorbed on the catalyst surface after long cycling, which results in electrode poisoning and poor electrode stability.[36] More importantly, all the electrodes achieved strong stability for approximately 90 cycles (Pd₁Pt_{2.9}/GA/NF and Pd₁Pt_{1.03}/GA/NF) to 240 cycles (Pd₁Pt_{1.31}/GA/NF) throughout 1248 cycles operations after the electrodes were fully activated (Tables S3-S5). The overall results show that the Pd₁Pt_{1.03}/GA/NF electrode has the highest activity and stability. More importantly, in a similar work, only 500 cycles of CV scanning were used to explore the stability of 2D graphene (Au-Ag/RGO/GC) in electrooxidation of glucose.[36] In contrast, the stability of the Pd₁Pt_x/GA/NF electrodes were evaluated up to 1248 cycles, in which the electrodes showed a good stability in the range of 90-150 cycles after the electrodes were activated (Table S3-S5). The small peak current density variation of the Pd₁Pt_x/GA/NF electrodes showed a good strength of the binder-free electrodes in glucose electrooxidation.

4. Conclusion

In summary, the Pd-Pt/GA/NF electrodes with different Pd/Pt ratios showed satisfactory performance in glucose electrooxidation in alkaline media. The catalytic activity of glucose electrooxidation was significantly affected by the Pd/Pt ratio in the electrodes under the tested conditions. The Pd₁Pt_{1.03}/GA/NF electrode showed a good electrocatalytic performance in 300 mM glucose/1 M NaOH solution in the prolong operation, which can be a good candidate for heavy duty glucose electrooxidation.

Acknowledgement

This study was supported by the Science and Technology Development Fund of the Macau SAR (FDCT-098/2015/A3), the Multi-Year Research Grants from the

Research & Development Office at the University of Macau (MYRG2017-00216-FST), and the UEA funding.

References

- [1] Pasta M, Hu LB, La Mantia F, Cui Y. Electrodeposited gold nanoparticles on carbon nanotube-textile: Anode material for glucose alkaline fuel cells. *Electrochemistry Communications*. 2012;19:81-4.
- [2] Brouzgou A, Yan LL, Song SQ, Tsiakaras P. Glucose electrooxidation over Pd_xRh/C electrocatalysts in alkaline medium. *Appl Catal B-Environ*. 2014;147:481-9.
- [3] Li L, Scott K, Yu EH. A direct glucose alkaline fuel cell using MnO₂-carbon nanocomposite supported gold catalyst for anode glucose oxidation. *J Power Sources*. 2013;221:1-5.
- [4] Tung SP, Huang TK, Lee CY, Chiu HT. Electrochemical growth of gold nanostructures on carbon paper for alkaline direct glucose fuel cell. *RSC Adv*. 2012;2:1068-73.
- [5] Yan XL, Ge XB, Cui SZ. Pt-decorated nanoporous gold for glucose electrooxidation in neutral and alkaline solutions. *Nanoscale Res Lett*. 2011;6.
- [6] An L, Zhao TS, Shen SY, Wu QX, Chen R. Alkaline direct oxidation fuel cell with non-platinum catalysts capable of converting glucose to electricity at high power output. *J Power Sources*. 2011;196:186-90.
- [7] Huang HJ, Wang X. Pd nanoparticles supported on low-defect graphene sheets: for use as high-performance electrocatalysts for formic acid and methanol oxidation. *J Mater Chem*. 2012;22:22533-41.
- [8] Zhu FC, Ma GS, Bai ZC, Hang RQ, Tang B, Zhang ZH, et al. High activity of carbon nanotubes supported binary and ternary Pd-based catalysts for methanol, ethanol and formic acid electro-oxidation. *J Power Sources*. 2013;242:610-20.
- [9] Li RS, Mao H, Zhang JJ, Huang T, Yu AS. Rapid synthesis of porous Pd and PdNi catalysts using hydrogen bubble dynamic template and their enhanced catalytic performance for methanol electrooxidation. *J Power Sources*. 2013;241:660-7.
- [10] Yang X, Yang QD, Xu J, Lee CS. Bimetallic PtPd nanoparticles on Nafion-graphene film as catalyst for ethanol electro-oxidation. *J Mater Chem*. 2012;22:8057-62.
- [11] Yang J, Tian C, Wang L, Fu H. An effective strategy for small-sized and highly-dispersed palladium nanoparticles supported on graphene with excellent performance for formic acid oxidation. *J Mater Chem*. 2011;21:3384-90.
- [12] Maiyalagan T, Dong XC, Chen P, Wang X. Electrodeposited Pt on three-dimensional interconnected graphene as a free-standing electrode for fuel cell

- application. *J Mater Chem.* 2012;22:5286-90.
- [13] Becerik I. The role of electrolytically co-deposited platinum-palladium electrodes on the electrooxidation of D. glucose in alkaline medium: A synergistic effect. *Turkish Journal of Chemistry.* 1999;23:57-66.
- [14] Becerik I, Suzer S, Kadirgan F. Platinum-palladium loaded polypyrrole film electrodes for the electrooxidation of D-glucose in neutral media. *Journal of Electroanalytical Chemistry.* 1999;476:171-6.
- [15] Yan LL, Brouzgou A, Meng YZ, Xiao M, Tsiakaras P, Song SQ. Efficient and poison-tolerant Pd_xAu_y/C binary electrocatalysts for glucose electrooxidation in alkaline medium. *Appl Catal B-Environ.* 2014;150-151:268-74.
- [16] Basu D, Basu S. Performance studies of Pd-Pt and Pt-Pd-Au catalyst for electro-oxidation of glucose in direct glucose fuel cell. *Int J Hydrog Energy.* 2012;37:4678-84.
- [17] Chen XM, Tian XT, Zhao LM, Huang ZY, Oyama M. Nonenzymatic sensing of glucose at neutral pH values using a glassy carbon electrode modified with graphene nanosheets and Pt-Pd bimetallic nanocubes. *Microchimica Acta.* 2014;181:783-9.
- [18] Sui Z, Zhang X, Lei Y, Luo Y. Easy and green synthesis of reduced graphite oxide-based hydrogels. *Carbon.* 2011;49:4314-21.
- [19] Zhu Y, Murali S, Stoller MD, Ganesh KJ, Cai W, Ferreira PJ, et al. Carbon-Based Supercapacitors Produced by Activation of Graphene. *Science.* 2011;332:1537-41.
- [20] Liu Z, Xu JK, Yue RR, Yang TT, Gao L. Facile one-pot synthesis of Au-PEDOT/rGO nanocomposite for highly sensitive detection of caffeic acid in red wine sample. *Electrochim Acta.* 2016;196:1-12.
- [21] Wu GH, Wu YF, Liu XW, Rong MC, Chen XM, Chen X. An electrochemical ascorbic acid sensor based on palladium nanoparticles supported on graphene oxide. *Anal Chim Acta.* 2012;745:33-7.
- [22] Wei J, Zang ZG, Zhang YB, Wang M, Du JH, Tang XS. Enhanced performance of light-controlled conductive switching in hybrid cuprous oxide/reduced graphene oxide (Cu₂O/rGO) nanocomposites. *Opt Lett.* 2017;42:911-4.
- [23] Kim SH, Jeong GH, Choi D, Yoon S, Jeon HB, Lee SM, et al. Synthesis of noble metal/graphene nanocomposites without surfactants by one-step reduction of metal salt and graphene oxide. *J Colloid Interface Sci.* 2013;389:85-90.
- [24] Gao YJ, Ma D, Wang CL, Guan J, Bao XH. Reduced graphene oxide as a catalyst for hydrogenation of nitrobenzene at room temperature. *Chem Commun.* 2011;47:2432-4.
- [25] Zang ZG, Zeng XF, Wang M, Hu W, Liu CR, Tang XS. Tunable photoluminescence of water-soluble AgInZnS-graphene oxide (GO) nanocomposites and their application in-vivo bioimaging. *Sens Actuator B-Chem.* 2017;252:1179-86.

- [26] Lee H, Choi TK, Lee YB, Cho HR, Ghaffari R, Wang L, et al. A graphene-based electrochemical device with thermoresponsive microneedles for diabetes monitoring and therapy. *Nat Nanotechnol.* 2016;11:566-72.
- [27] Li J, Liu C-y, Liu Y. Au/graphene hydrogel: synthesis, characterization and its use for catalytic reduction of 4-nitrophenol. *J Mater Chem.* 2012;22:8426-30.
- [28] Jeong GH, Kim SH, Kim M, Choi D, Lee JH, Kim JH, et al. Direct synthesis of noble metal/graphene nanocomposites from graphite in water: photo-synthesis. *Chem Commun.* 2011;47:12236-8.
- [29] Jin Z, Nackashi D, Lu W, Kittrell C, Tour JM. Decoration, Migration, and Aggregation of Palladium Nanoparticles on Graphene Sheets. *Chem Mat.* 2010;22:5695-9.
- [30] Wang H, Wang G, Ling Y, Qian F, Song Y, Lu X, et al. High power density microbial fuel cell with flexible 3D graphene-nickel foam as anode. *Nanoscale.* 2013;5:10283-90.
- [31] Tsang C-HA, Hui KN, Hui KS, Ren L. Deposition of Pd/graphene aerogel on nickel foam as a binder-free electrode for direct electro-oxidation of methanol and ethanol. *J Mater Chem A.* 2014;2:17986-93.
- [32] Yi QF, Yu WQ, Niu FJ. Novel Nanoporous Binary Au-Ru Electrocatalysts for Glucose Oxidation. *Electroanalysis.* 2010;22:556-63.
- [33] Wu XF, Li RY, Li ZJ. Synthesis of gold nanoclusters/glucose oxidase/graphene oxide multifunctional catalyst with surprisingly enhanced activity and stability and its application for glucose detection. *RSC Adv.* 2014;4:9935-41.
- [34] Joshi AC, Markad GB, Haram SK. Rudimentary simple method for the decoration of graphene oxide with silver nanoparticles: Their application for the amperometric detection of glucose in the human blood samples. *Electrochim Acta.* 2015;161:108-14.
- [35] Wang Q, Cui X, Guan W, Zheng W, Chen J, Zheng X, et al. Synthesis of flower-shape palladium nanostructures on graphene oxide for electrocatalytic applications. *Journal of Physics and Chemistry of Solids.* 2013;74:1470-4.
- [36] Shi QF, Diao GW, Mu SL. The electrocatalytic oxidation of glucose on the bimetallic Au-Ag particles-modified reduced graphene oxide electrodes in alkaline solutions. *Electrochim Acta.* 2014;133:335-46.
- [37] Kovtyukhova NI, Ollivier PJ, Martin BR, Mallouk TE, Chizhik SA, Buzaneva EV, et al. Layer-by-layer assembly of ultrathin composite films from micron-sized graphite oxide sheets and polycations. *Chem Mat.* 1999;11:771-8.
- [38] Zhao JW, Shao MF, Yan DP, Zhang ST, Lu ZZ, Li ZX, et al. A hierarchical heterostructure based on Pd nanoparticles/layered double hydroxide nanowalls for enhanced ethanol electrooxidation. *J Mater Chem A.* 2013;1:5840-6.

- [39] Sawangphruk M, Krittayavathananon A, Chinwipas N. Ultraporous palladium on flexible graphene-coated carbon fiber paper as high-performance electro-catalysts for the electro-oxidation of ethanol. *J Mater Chem A*. 2013;1:1030-4.
- [40] Spets JP, Lampinen MJ, Kiros Y, Rantanen J, Anttila T. Direct Glucose Fuel Cell with the Anion Exchange Membrane in the Near-Neutral-State Electrolyte. *International Journal of Electrochemical Science*. 2012;7:11696-705.
- [41] Das D, Ghosh S, Basumallick I. Electrochemical Studies on Glucose Oxidation in an Enzymatic Fuel Cell with Enzyme Immobilized on to Reduced Graphene Oxide Surface. *Electroanalysis*. 2014;26:2408-18.
- [42] Cai ZX, Liu CC, Wu GH, Chen XM, Chen X. Palladium nanoparticles deposit on multi-walled carbon nanotubes and their catalytic applications for electrooxidation of ethanol and glucose. *Electrochim Acta*. 2013;112:756-62.
- [43] Kim Y, Noh Y, Lim EJ, Lee S, Choi SM, Kim WB. Star-shaped Pd@Pt core-shell catalysts supported on reduced graphene oxide with superior electrocatalytic performance. *J Mater Chem A*. 2014;2:6976-86.
- [44] Chen XM, Cai ZX, Chen X, Oyama M. Green synthesis of graphene-PtPd alloy nanoparticles with high electrocatalytic performance for ethanol oxidation. *J Mater Chem A*. 2014;2:315-20.
- [45] Lim HN, Huang NM, Lim SS, Harrison I, Chia CH. Fabrication and characterization of graphene hydrogel via hydrothermal approach as a scaffold for preliminary study of cell growth. *Int J Nanomed*. 2011;6:1817-23.
- [46] Ozturk Z, Sen F, Sen S, Gokagac G. The preparation and characterization of nano-sized Pt-Pd/C catalysts and comparison of their superior catalytic activities for methanol and ethanol oxidation. *J Mater Sci*. 2012;47:8134-44.
- [47] Pacley S, Mitchel W, Murray PT, Anderson D, Smith HE, Beck-Millerton E, et al. Investigation of the behavior of the Ni catalyst in chemical vapor deposition synthesis of carbon nanopearls. In: Pribat D, Lee YH, Razeghi M, editors. *Carbon Nanotubes, Graphene, and Associated Devices V*. Bellingham: Spie-Int Soc Optical Engineering; 2012.
- [48] Yi Q, Niu F, Yu W. Pd-modified TiO₂ electrode for electrochemical oxidation of hydrazine, formaldehyde and glucose. *Thin Soild Films*. 2011;519:3155-61.

Figure captions

Fig 1. SEM image of (a) NF and (b) Pd₁Pt_{2.9}/GA/NF (95×, scale bar: 200 μm), and magnified image of (a) at (c) 1000× (red circle area of (b), scale bar: 100 μm), and (d) 5500× (red circle area of (c), scale bar: 5 μm), and (e) EDX survey of Pd₁Pt_{2.9}/GA/NF.

Fig 2. TEM image of (a) Pd₁Pt_{2.9}/GA (Scale bar: 1 μm), and (b) magnified image of (a) (red circle area of (a), scale bar: 20 nm), and (c) SAED pattern of the particle in (b).

Fig 3. XPS spectra of (a) Pd3d, (b) Pt4f, (c) C1s, and (d) Ni2p of Pd₁Pt_{2.9}/GA/NF, and (e) C1s of raw GO.

Fig 4. CV curves of (a) Pd₁Pt_{2.9}/GA/NF, Pd₁Pt_{1.31}/GA/NF, and Pd₁Pt_{1.03}/GA/NF compared with monometallic Pt and Pd in 30 mM glucose/0.1 M NaOH solution at 25th cycle, and (b) its expanded view excluding Pd₁Pt_{1.03}/GA/NF electrode.

Fig 5. Combined CV curves of (a) Pd₁Pt_{2.9}/GA/NF, (b) Pd₁Pt_{1.31}/GA/NF, and (c) Pd₁Pt_{1.03}/GA/NF in 75 mM glucose/0.1 M NaOH and 75 mM glucose/1 M NaOH solution.

Fig 6. CV curves of (a) Pd₁Pt_{2.9}/GA/NF, (b) Pd₁Pt_{1.31}/GA/NF, and (c) Pd₁Pt_{1.03}/GA/NF in 75 mM, 300 mM and 500 mM glucose/1 M NaOH solution.

Fig 7. CV curves of (a) Pd₁Pt_{2.9}/GA/NF, (b) Pd₁Pt_{1.31}/GA/NF, and (c) Pd₁Pt_{1.03}/GA/NF in 30 mM and 75 mM glucose/0.1 M NaOH solution

Fig 8. CV curves of (a) Pd₁Pt_{2.9}/GA/NF, (b) Pd₁Pt_{1.31}/GA/NF, (c) Pd₁Pt_{1.03}/GA/NF, and (d) variation of J_{a2} potential of Pd-Pt/GA/NF electrodes in 300 mM glucose/1 M NaOH solution throughout 1248 cycles scanning.

Table captions

Table 1. Variation of J_f (a_1, a_2 : $A \text{ g}^{-1}$) under different combinations of glucose and NaOH concentration (0.1 M and 1 M) in the 25th cycle of electrooxidation.

Figures

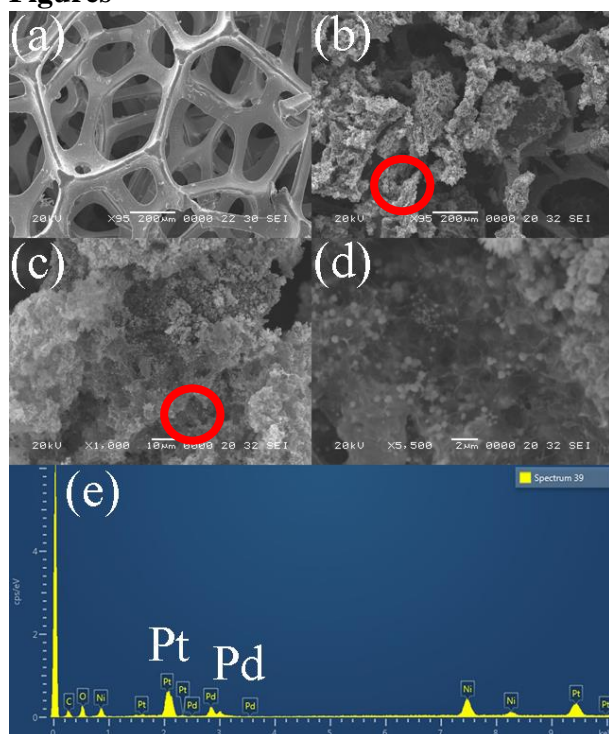


Fig 1. SEM image of (a) NF and (b) Pd₁Pt_{2.9}/GA/NF (95×, scale bar: 200 μm), and magnified image of (a) at (c) 1000× (red circle area of (b), scale bar: 100 μm), and (d) 5500× (red circle area of (c), scale bar: 5 μm), and (e) EDX survey of Pd₁Pt_{2.9}/GA/NF.

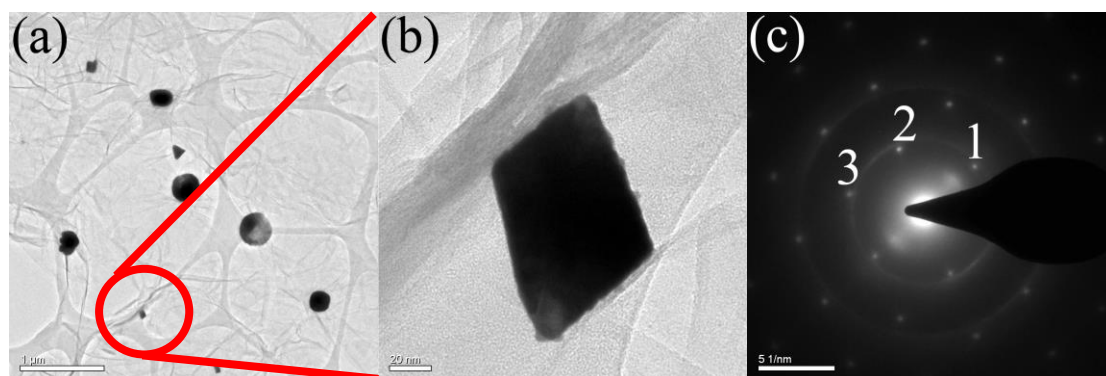


Fig 2. TEM image of (a) Pd₁Pt_{2.9}/GA (Scale bar: 1 μm), and (b) magnified image of (a) (red circle area of (a), scale bar: 20 nm), and (c) SAED pattern of the particle in (b).

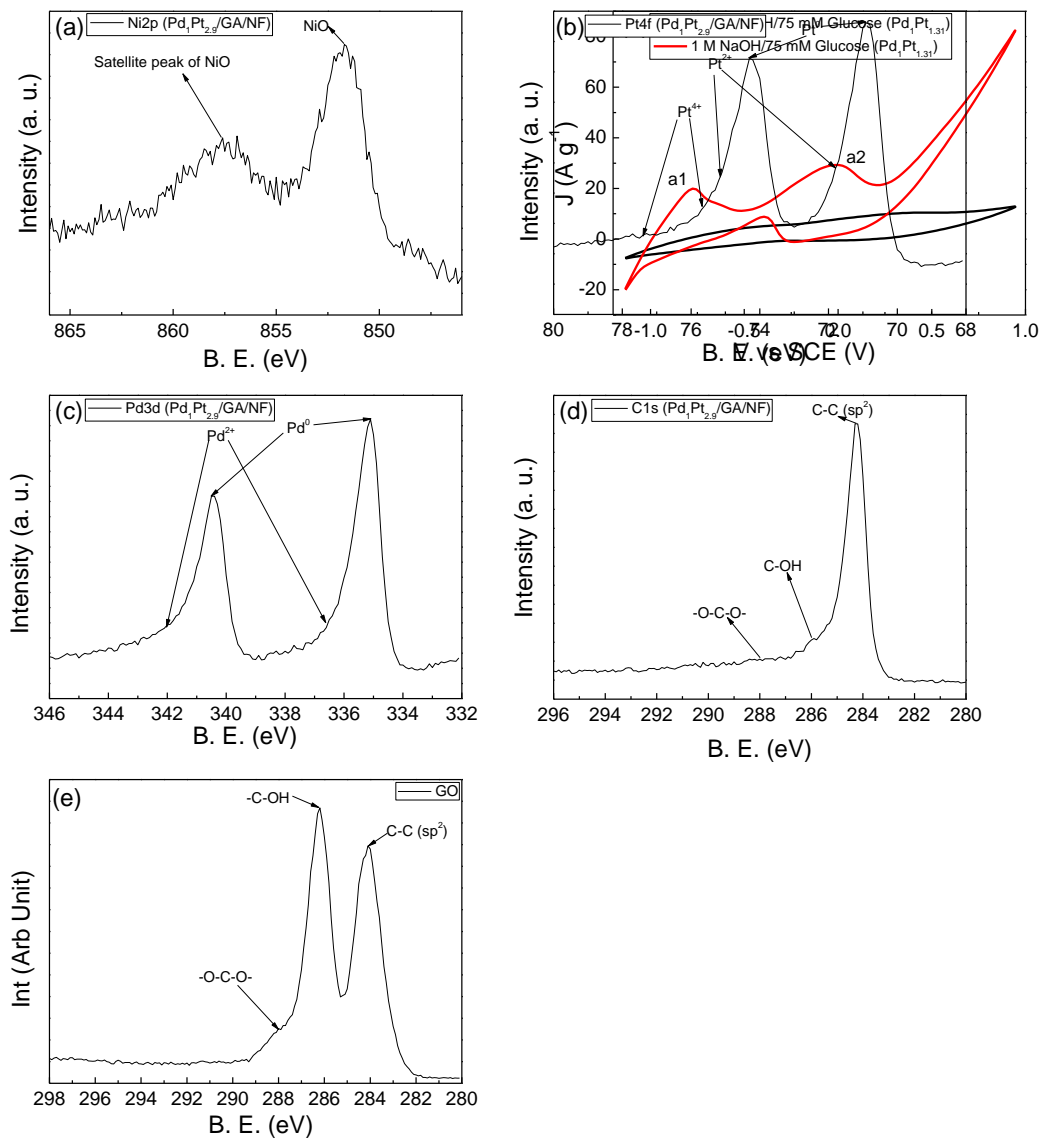


Fig 3. XPS spectra of (a) Pd_{3d}, (b) Pt_{4f}, (c) C_{1s}, and (d) Ni_{2p} of Pd₁Pt_{2.9}/GA/NF, and (e) C_{1s} of raw GO.

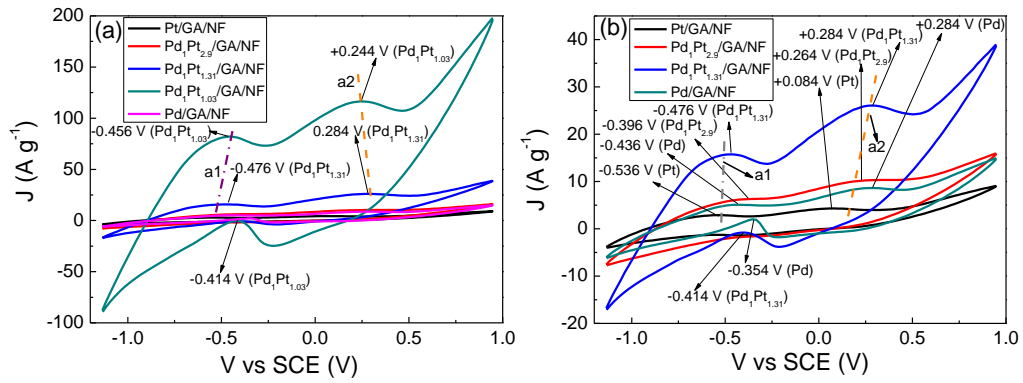


Fig 4. CV curves of (a) Pd₁Pt_{2.9}/GA/NF, Pd₁Pt_{1.31}/GA/NF, and Pd₁Pt_{1.03}/GA/NF compared with monometallic Pt and Pd in 30 mM glucose/0.1 M NaOH solution at 25th cycle, and (b) its expanded view excluding Pd₁Pt_{1.03}/GA/NF electrode.

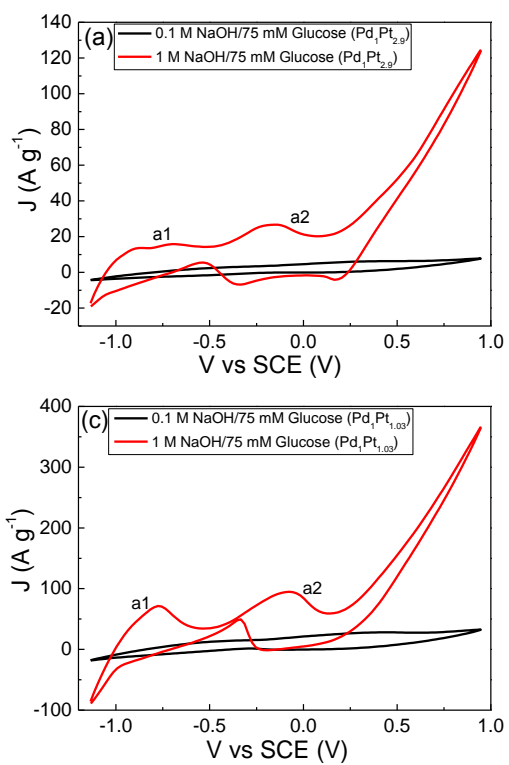


Fig 5. Combined CV curves of (a) $\text{Pd}_1\text{Pt}_{2.9}/\text{GA}/\text{NF}$, (b) $\text{Pd}_1\text{Pt}_{1.31}/\text{GA}/\text{NF}$, and (c) $\text{Pd}_1\text{Pt}_{1.03}/\text{GA}/\text{NF}$ in 75 mM glucose/0.1 M NaOH and 75 mM glucose/1 M NaOH solution.

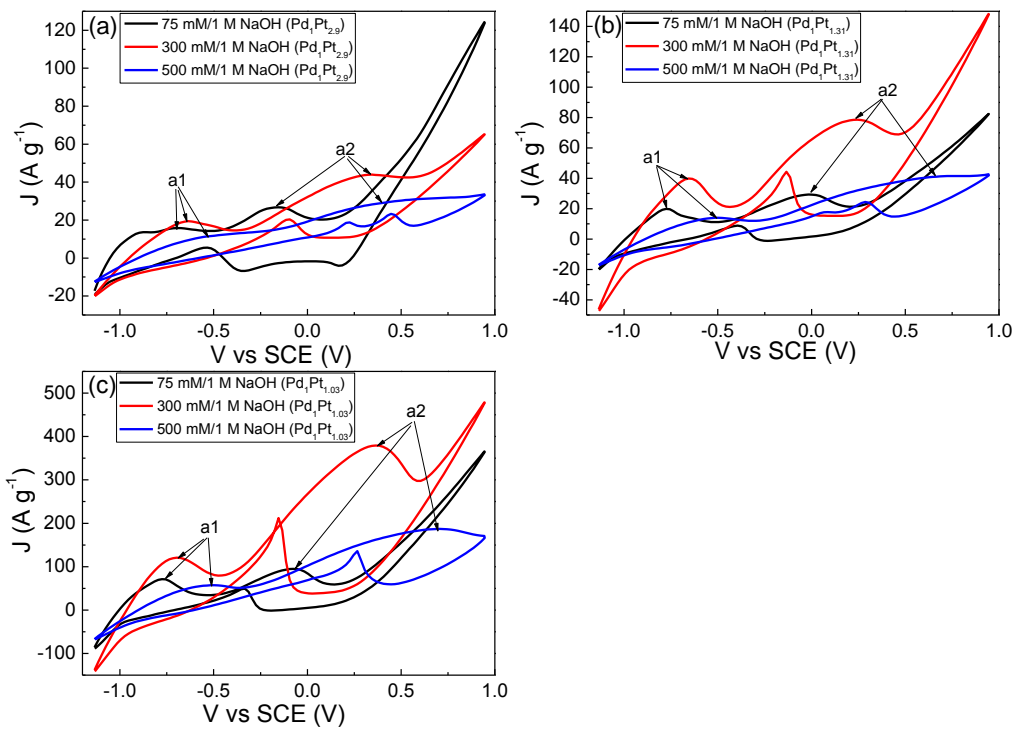


Fig 6. CV curves of (a) Pd₁Pt_{2.9}/GA/NF, (b) Pd₁Pt_{1.31}/GA/NF, and (c) Pd₁Pt_{1.03}/GA/NF

in 75 mM, 300 mM and 500 mM glucose/1 M NaOH solution.

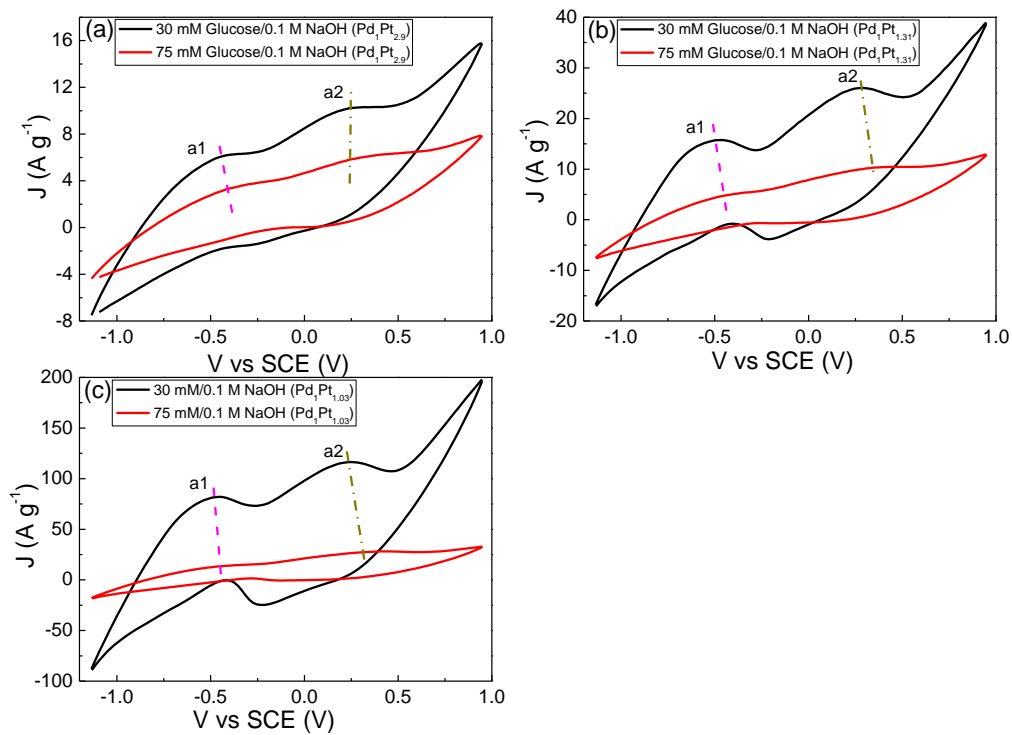


Fig 7. CV curves of (a) Pd₁Pt_{2.9}/GA/NF, (b) Pd₁Pt_{1.31}/GA/NF, and (c)

Pd₁Pt_{1.03}/GA/NF in 30 mM and 75 mM glucose/0.1 M NaOH solution.

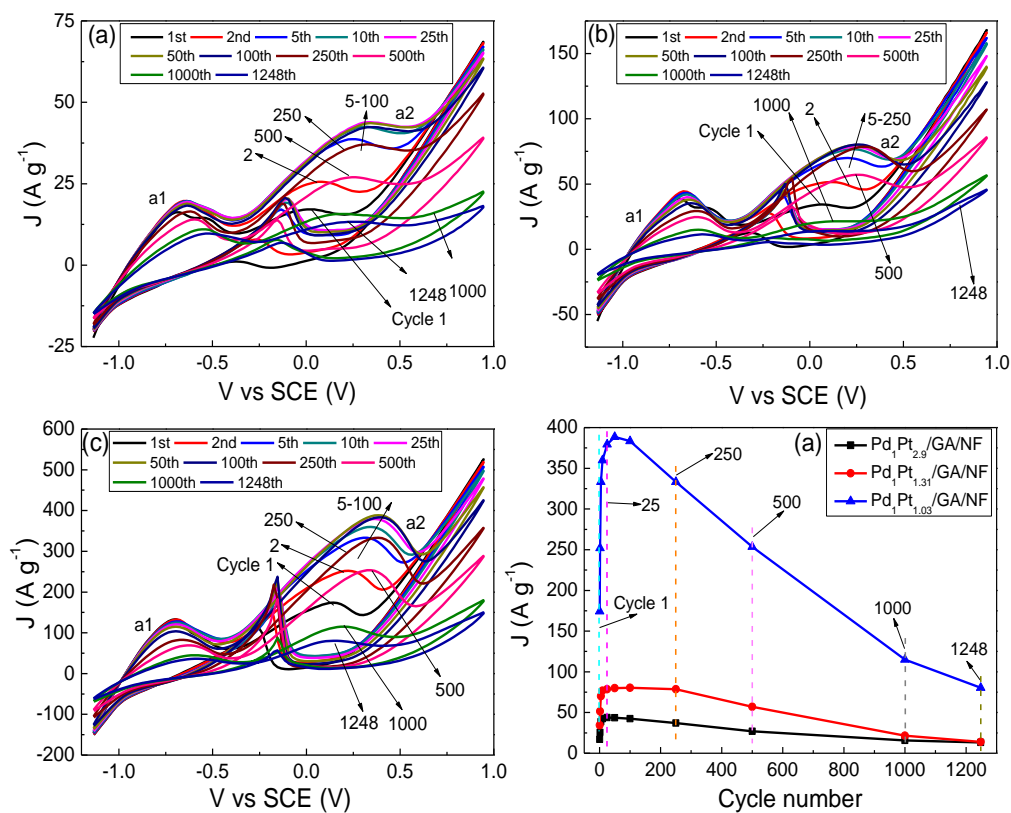


Fig 8. CV curves of (a) Pd₁Pt_{2.9}/GA/NF, (b) Pd₁Pt_{1.31}/GA/NF, (c) Pd₁Pt_{1.03}/GA/NF, and (d) variation of J_{fa2} potential of Pd-Pt/GA/NF electrodes in 300 mM glucose/1 M NaOH solution throughout 1248 cycles scanning.

Table 1 Variation of J_f (a1, a2: $A g^{-1}$) under different combinations of glucose and

NaOH concentration (0.1 M and 1 M) in the 25th cycle of electrooxidation.

NaOH/Glucose concentration (Cycle)	Pd ₁ Pt _{2.9} /GA/NF		Pd ₁ Pt _{1.31} /GA/NF		Pd ₁ Pt _{1.03} /GA/NF	
	J_f (a1)	J_f (a2)	J_f (a1)	J_f (a2)	J_f (a1)	J_f (a2)
0.1 M/30 mM (25)	6.24	10.26	15.74	26.06	82.02	116.4
0.1 M/75 mM (25)	2.84	6.2	4.86	10.46	13.33	28.01
1 M/75 mM (25)	15.83	26.75	19.9	29.3	71.33	94.78
1 M/300 mM (25)	13.4	43.9	39.9	78.6	120.7	379.4
1 M/500 mM (25)	11.06	28.52	14.01	41.36	57.19	186.9